

Quantification of plasmon excitations in core-level photoemission

F. Yubero¹ and S. Tougaard²

¹*Inst. de Ciencia de Materiales de Sevilla (CSIC-U. Sevilla), Américo Vespucio s/n, E-41092 Sevilla, Spain*

²*Physics Institute, University of Southern Denmark (SDU), DK-5230 Odense M, Denmark*

(Received 29 April 2004; published 13 January 2005)

Calculation of photoelectron spectra (PES) based on our previous dielectric response model [A. C. Simonsen *et al.* Phys. Rev. B **56**, 1612 (1997)] for electronic excitations in PES are compared with recently reported experimental data. It is found that the dielectric description of electron energy losses in photoemission reproduces quantitatively the angular dependence of the surface and bulk electron losses observed experimentally for the Al2s photoemission spectra of Al(111), excited with MgK α radiation. The model also allows to calculate the separate intrinsic and extrinsic effects in photoemission. Thus, the extrinsic losses account for more than 95% of the total surface excitations. Regarding the bulk excitations, both extrinsic and intrinsic contributions vary significantly with emission angle. The intrinsic contribution represents $\sim 35\%$ of the intensity at the bulk plasmon position at normal emission while only 18% at 80° glancing emission. The calculations presented here can easily be used to interpret PES spectra of other materials in terms of intrinsic and extrinsic effects, if their dielectric properties are known.

DOI: 10.1103/PhysRevB.71.045414

PACS number(s): 82.80.Pv, 73.20.Mf, 79.60.Bm

I. INTRODUCTION

Photoelectron spectroscopy (PES) has over the last three decades become a standard technique for surface analysis. It is used routinely to identify electronic effects at surfaces or for elemental quantification purposes. In spite of the widespread use of the technique, some fundamental aspects regarding the interpretation of the photoemission spectra remain uncertain.

The simplest interpretation of photoemission spectra is based on the “sudden approximation” considering a one-electron wave function. However, the well known appearance of shake-up effects and plasmon excitations in PES cannot be appropriately described within this simple picture. Thus, in general, many-body effects and surface effects are important to describe the observed energy distribution in PES.^{1–18} Several models have been proposed in the past for evaluation of PES spectral line shapes.^{2,8,11,14,16–22} Most models are based on a quantum-mechanical description of the perturbation induced by the photoexcitation process of the electronic states of the solid. With these models it is difficult to compare between theory and experiment for materials other than those showing free electronlike behavior. Reviews on this subject were recently reported by Hedin *et al.*^{19,20}

It is well known that the energy loss structure in PES can originate from both the static core hole created during the photoexcitation of the core electron and by the excitations that take place during the transport of the photoelectron out of the solid. The corresponding terms are usually called “intrinsic” and “extrinsic” excitations.

Inspired by recent investigations^{20,21} of the extrinsic and intrinsic contribution to surface and bulk plasmon excitations in photoelectron spectra, we have made model calculations of experimental PES spectra using our semiclassical model.²² In this model, the interaction of the medium with the core hole and the effect of the surface are described by the complex dielectric function of the medium (i.e., it is assumed that

the dielectric function is known and all interactions and excitations are calculated from this). The model takes into account energy loss from the core hole, the moving electron, the surface, as well as the energy loss that takes place in the vacuum after the electron has left the solid surface. A clear advantage of the dielectric response description we have developed over the quantum mechanical models, is that extensions beyond materials that can be described by the nearly free electron model are straightforward. This is of paramount importance for practical applications because very few materials are well described within the free electron model.

Based on a similar dielectric response approach we proposed a model to simulate spectra in a reflection electron energy loss (REELS) experiment.^{23,26} The validity of this model has been tested thoroughly in many experiments^{24,25,27–31} including different classes of materials (metals, oxides, semiconductors), different energies and different experimental geometries. In general a good agreement was found between the REELS model calculations and the experiments. The model for the simulation of PES spectral line shapes has not been investigated to the same extent. Therefore, in the present paper, we have tested the ability of the PES theory in Ref. 22 to account for the peak shape by comparison to the experiments published by Biswas *et al.*²¹ for angular dependence of Al2s and Al2p emission. Aluminum is a well suited material to test the validity of the model because it shows distinguished surface and bulk plasmon structure. The experiments performed by Biswas *et al.*²¹ are done on clean well characterized Al surfaces. The samples used in Ref. 21 are also very flat. The latter is extremely important for measurements at glancing emission angles where surface roughness will influence the interaction of the electron with the surface. We calculate the line shape of the Al2s photoelectron peak as a function of the angle of emission. In general we find that there is a good quantitative agreement between the calculations based on our dielectric response model for PES (Ref. 22) and the experiments. In addition, we have also calculated the relative contribution of

intrinsic plasmon excitations to the PES spectra as a function of angle of emission.

II. THEORY

In a previous paper²² we developed a semiclassical model based on a dielectric description of the electron energy losses of a photon excited core electron. It is assumed that an electron core-hole pair (both considered as point charges) is created at a given depth inside a semi-infinite medium, characterized by a dielectric function $\varepsilon(k, \omega)$. The calculation applies the “specular reflection model”^{32,33} which allows one to solve the electrodynamic problem with the proper boundary conditions for the electric potential and field at the surface-vacuum interface. The core-hole is assumed to be static with infinite lifetime, i.e., it remains at a fixed location forever after its creation at time $t=0$. The photoelectron escapes from the semiinfinite medium with a velocity \mathbf{v} in a rectilinear trajectory. Within this model, we define an effective inelastic scattering cross section $K_{\text{eff}}(E_0, \hbar\omega; \varepsilon, \theta, a)$ in terms of the induced potential. $K_{\text{eff}}(E_0, \hbar\omega; \varepsilon, \theta, a)$ is defined as the average probability that a photoelectron excited at depth a with energy E_0 shall lose energy $\hbar\omega$ per unit energy loss and per unit path length while traveling in the specified geometry. The average is over the path length $x=a/\cos\theta$, where θ is the angle to the surface normal. Neglecting angular electron deflection one gets²²

$$K_{\text{eff}}(E_0, \hbar\omega; \varepsilon, \theta, a) = \frac{2}{(2\pi)^4 \hbar^2 \omega X} \text{Re} \left\{ \int dt \int d^3r \rho_e(\mathbf{r}, t) i \times \int d^3k \mathbf{k} \cdot \mathbf{v} \Phi_{\text{ind}}(\mathbf{k}, \omega; \varepsilon, \theta, a) e^{i(kr - \omega t)} \right\}, \quad (1)$$

where \mathbf{r} is the position, $\rho_e(\mathbf{r}, t)$ the charge density of the escaping photoelectron, and $\Phi_{\text{ind}}(\mathbf{k}, \omega; \varepsilon, \theta, a)$ the Fourier transform of the potential induced by the escaping photoelectron and the static core hole in the semiinfinite medium. Equation (1) includes all energy loss processes, i.e., intrinsic, extrinsic, and interference losses, and losses due to the effect of the surface and during the transport in the vacuum. The so called interference terms are included as an integral part of the formalism. Thus, the induced potential in Eq. (1) includes all effects including the interference between the fields set up by the hole and the moving photoelectron. It also includes terms that are due to interference terms that arise from the boundary conditions for the fields and the potentials at the surface as well as interactions that take place when the electron moves in the vacuum outside the solid surface.

As may be seen in Ref. 22, the final expression for $\Phi_{\text{ind}}(\mathbf{k}, \omega; \varepsilon, \theta, a)$ has several terms which, from their dependence on the charge of the static hole, can formally be identified as being due to the static core hole (which we denote “hole” terms) and the rest which are independent of the hole (which we denote “no-hole” terms) so that

$$\Phi_{\text{ind}}(\mathbf{k}, \omega; \varepsilon, \theta, a) = \Phi_{\text{ind, no-hole}}(\mathbf{k}, \omega; \varepsilon, \theta, a) + \Phi_{\text{ind, hole}}(\mathbf{k}, \omega; \varepsilon, \theta, a). \quad (2)$$

This is a formal division and it is not strictly possible to make this distinction because the different contributions interfere. More details and the precise expressions for the “no-hole” and “hole” contribution to the total induced potential can be found in Ref. 22. The expressions are quite involved and will not be repeated here. In this paper we shall define “intrinsic” excitations as those that are due to the potential $\Phi_{\text{ind, hole}}$ and “extrinsic” excitations as those that are due to the potential $\Phi_{\text{ind, no-hole}}$. With this identification the total cross section is decomposed in the form

$$K_{\text{eff}}(E_0, \hbar\omega; \varepsilon, \theta, a) = K_{\text{eff}}^{\text{extrinsic}}(E_0, \hbar\omega; \varepsilon, \theta, a) + K_{\text{eff}}^{\text{intrinsic}}(E_0, \hbar\omega; \varepsilon, \theta, a), \quad (3)$$

where $K_{\text{eff}}^{\text{intrinsic}}(E_0, \hbar\omega; \varepsilon, \theta, a)$ is the sum of the terms that would disappear if the hole were not there and $K_{\text{eff}}^{\text{extrinsic}}(E_0, \hbar\omega; \varepsilon, \theta, a)$ is the sum of the remaining terms. Note that with this separation in “intrinsic” and “extrinsic” excitations, they include the so called “interference” effects that may be attributed to the interference between the fields from the core hole and the moving electron. Since the interference effect diminishes the total energy loss, the intrinsic cross section may be negative (see Fig. 2). The total cross section is, however, always positive. Thus, within this model, it is possible to evaluate quantitatively extrinsic and intrinsic contributions to the photoelectron energy losses if the dielectric properties of the media, the primary kinetic energy and exit angle are known.

The properties of the electronic states of the material are described by the complex dielectric function of the medium where the electron is traveling. We apply an expansion^{24,34}

$$\text{Im} \left\{ \frac{1}{\varepsilon(k, \hbar\omega)} \right\} = \theta(\hbar\omega - E_g) \sum_{i=1}^n \frac{A_i \gamma_i \hbar\omega}{\left(\left(\hbar\omega_{0i} + \alpha_i \frac{\hbar^2 k^2}{2m} \right)^2 - \hbar\omega^2 \right)^2 + (\gamma_i \hbar\omega)^2}, \quad (4)$$

where A_i , γ_i , and $\hbar\omega_{0i}$ is the oscillator strength, width and energy position of the i th oscillator. The dispersion for each oscillator is α_i . For a free-electron-like material such as Al, $\alpha_i=1$. The step function $\theta(\hbar\omega - E_g)$ is included to simulate a possible energy gap E_g .

In an experimental PES measurement, there will be contributions from photoelectrons excited at a range of depths. It is therefore necessary to account for their relative contributions to the spectrum. This can be done by introducing an averaged effective cross section

$$K_{\text{eff, av}}(E_0, \hbar\omega; \varepsilon, \theta) = K_{\text{eff, av}}^{\text{extrinsic}}(E_0, \hbar\omega; \varepsilon, \theta) + K_{\text{eff, av}}^{\text{intrinsic}}(E_0, \hbar\omega; \varepsilon, \theta), \quad (5)$$

where the “extrinsic” and “intrinsic” contributions can be estimated as weighted average over the total pathlength x

traveled by the electron inside the medium as

$$K_{\text{eff,av}}^{\text{extrinsic/intrinsic}}(E_0, \hbar\omega; \varepsilon, \theta) = \int_0^\infty W(E_0; \varepsilon, \theta, a) K_{\text{eff}}^{\text{extrinsic/intrinsic}}(E_0, \hbar\omega; \varepsilon, \theta, a) dx. \quad (6)$$

The weight function $W(E_0; \varepsilon, \theta, a)$ takes into account the path length distribution of the electrons having suffered only a single inelastic scattering event. For a homogeneous solid it is given by

$$W(E_0; \varepsilon, \theta, a) = \frac{x \exp[-x/\lambda_{\text{eff}}(E_0; \varepsilon, \theta, a)]}{\int_0^\infty x \exp[-x/\lambda_{\text{eff}}(E_0; \varepsilon, \theta, a)] dx}, \quad (7)$$

where $\lambda_{\text{eff}}(E_0; \varepsilon, \theta, a)$ is the inverse of the area of the corresponding cross section $K_{\text{eff}}(E_0, \hbar\omega; \varepsilon, \theta, a)$:

$$\lambda_{\text{eff}}(E_0; \varepsilon, \theta, a) = \left[\int_0^\infty K_{\text{eff}}(E_0, \hbar\omega; \varepsilon, \theta, a) d\hbar\omega \right]^{-1}. \quad (8)$$

$\lambda_{\text{eff}}(E_0; \varepsilon, \theta, a)$ is thus the inelastic mean free path for an electron starting at depth a towards the surface in direction θ traveling in a material described by the dielectric function ε . Note that $\lambda_{\text{eff}}(E_0; \varepsilon, \theta, a)$, in addition to the well-known dependence on the dielectric properties of the material, depends on both a and θ . This is a consequence of surface excitations as well as excitations that take place in the vacuum after the electron has left the surface.

In order to compare to photoemission experiments, the elastic peak must be included. If $F(E)$ is the primary excitation spectrum, the model spectrum $J(E)$ from a homogeneous sample corresponding to one inelastic scattering event is given by

$$J(E) \propto F(E) + \lambda \int_E^\infty F(E') K_{\text{eff,av}}(F_0, F' - E) dE', \quad (9)$$

where $E' - E = \hbar\omega$ and λ represents the inelastic mean free path of the considered electrons. In order to be self-consistent with the calculated $K_{\text{eff,av}}$, λ is taken as the inverse of the area of $K_{\text{eff,av}}$. Thus, $J(E)$ represents the model XPS spectrum corresponding to a zero-loss peak $F(E)$ together with the single inelastic scattering contribution. In practice, $F(E)$ can be taken as a mixed Gaussian-Lorentzian curve with a width given by the lifetime broadening of the excitation.

III. RESULTS AND DISCUSSION

In this section we compare our model calculations to experimental PES of Al2s core electrons taken from a Al(111).²¹ Figure 1 shows the model calculations of the spectra using Eq. (9). The inset shows the experimental data of Biswas *et al.*²¹ obtained under the same conditions. In particular, the experimental spectra were excited with MgK α radiation and recorded for several emission angles between

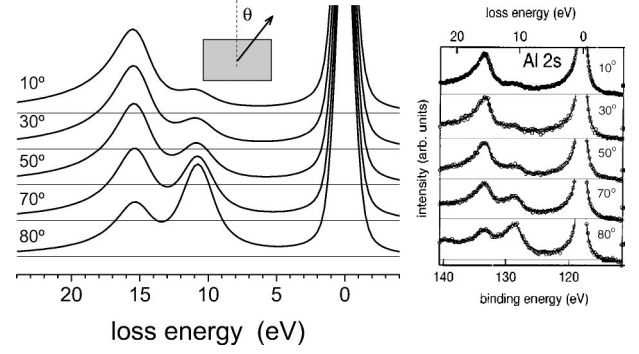


FIG. 1. Model photoemission spectra $J(E)$ containing the zero loss peak and the single inelastic scattering contributions, calculated according to Eq. (9) for photoelectrons traveling in Al with 1130 eV kinetic energy for several emission angles. Right: experimental results for Al2s photoemission in Al sample from Biswas *et al.* (Ref. 21) for the same experimental conditions used in the model calculations.

10° and 80°. The inputs in the model simulation are the following.

- The dielectric function $\varepsilon(k, \omega)$ of Al has been taken as in Eq. (4) with a single oscillator at $\hbar\omega_0 = 15.0$ eV with $\gamma = 1.5$ eV, $A = 225$ eV², $E_g = 0$ eV, and $\alpha = 1$. This dielectric function was previously found to account well for simulations of experimental REELS spectra at different primary electron energies.²³
- The primary energy $E_0 = 1130$ eV which is the kinetic energy of the MgK α excited Al2s electrons.
- The emission angle θ corresponding to each experiment.
- The full width at half maximum (FWHM) of the zero-loss peak $F(E)$, that has been chosen to fit the experimental peak. In particular we used in all cases an average of Gaussian and Lorentzian peak with 1.5 eV FWHM.

As expected, the relative contribution of surface to bulk losses increases for increasing glancing angles. This is seen for both model simulation and experiment. Note however that significant increase in the surface contribution to the spectra occur only for emission angle larger than 70°. From the results in Fig.1, it is clear that the present model calculations reproduces the absolute intensities as well as shapes of both bulk and surface excitations for the whole series of experimental spectra taken at exit angles from 10° to 80°.

It is worthwhile to note that the only fitting parameter in our model is the width of the elastic peak. The parameters that define the dielectric function are taken from independent experiments. Even the inelastic mean free path used in the calculations is obtained selfconsistently from the model as the inverse of the area of the corresponding cross section. The calculation scheme can easily be applied to other materials and experimental conditions. The only input in the calculations is the dielectric function which for a given solid may be taken from Ref. 35 or it may be determined experimentally from analysis of REELS spectra using the method in Ref. 23–26.

The successful description of the set of experiments in Fig. 1 gives confidence in the validity of the semiclassical

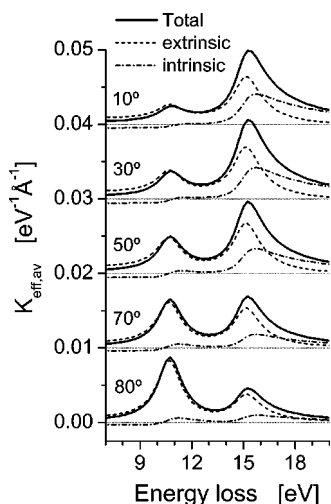


FIG. 2. Effective average cross sections $K_{\text{eff,av}}(E_0, \hbar\omega; \varepsilon, \theta)$ corresponding to the model calculations in Fig. 1. The extrinsic and intrinsic contributions to the spectra are indicated as dashed and dashed-dot lines, respectively.

dielectric model for PES. We have therefore applied the same model to also study the excitations in terms of extrinsic and intrinsic contributions to the measured spectra. As was discussed above, these contributions are related to the electronic excitations due to the moving electron or to the core-hole, respectively. When we now use the above definitions of intrinsic and extrinsic excitations, it is possible to calculate the relative contribution from these two types of excitations.

Figure 2 shows model calculations of $K_{\text{eff,av}}$ for photoelectrons of 1130 eV kinetic energy traveling in Al. The “extrinsic” and “intrinsic” contributions to the total $K_{\text{eff,av}}$ are included as dashed and dot-dashed lines, respectively. At this point we want to stress that the calculated “intrinsic” and “extrinsic” contributions come out from the model in Ref. 22 simply as loss terms during the photoelectron emission either induced by the presence of the hole or independent of it. As described above the slightly negative intrinsic cross sections in Fig. 2 is due to the “interference” effect which is included in the intrinsic cross section.

Figure 2 shows that both extrinsic and intrinsic surface losses are enhanced with respect to the corresponding bulk losses at glancing emission angles. However, the change with angle of emission in the absolute contribution of extrinsic and intrinsic losses to $K_{\text{eff,av}}$ is different. For the “surface” losses (identified as the region around the peak at ~ 10 eV), the “extrinsic” contribution to $K_{\text{eff,av}}$ accounts for more than 95% of the intensity for all studied angles of emission.

For the bulk losses (identified as the peak at ~ 15 eV and beyond) the relative intensity of “intrinsic” to “extrinsic” excitation varies with the emission angle. Figure 3 shows the percentage of intrinsic contribution to the bulk losses measured either by the area (full line) or by the height (dashed line) at the bulk plasmon position. The relative contribution of intrinsic losses to the bulk plasmons decreases with the angle of emission. Thus $\sim 62\%$ of the total area of the bulk plasmon is due to intrinsic losses at normal emission, while it is $\sim 35\%$ at 80° . If we just consider the height at the bulk plasmon energy (i.e., at 15.0 eV energy loss), $\sim 35\%$ of the

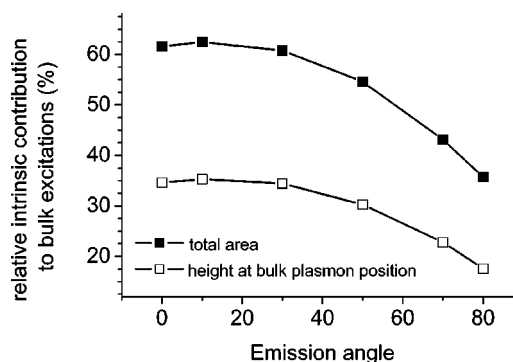


FIG. 3. Relative intrinsic contribution to the bulk plasmon intensity for photoelectrons traveling in Al with 1130 eV kinetic energy for several emission angles. Full and hollow squares refer to the total area and the height at the bulk plasmon position (i.e., 15.0 eV energy loss), respectively.

signal is intrinsic for normal emission and $\sim 18\%$ at 80° . For comparison, there is a large degree of discrepancy between estimations of intrinsic effect to photoemission in Al found by several authors. Thus, it has been reported that the intrinsic effects account for 10,⁸ 11,¹² 26,¹¹ 20–50,¹⁵ or 50 % (Ref. 2) of the total plasmon intensity.

The shape of the intrinsic losses is clearly different from the extrinsic. The intrinsic losses are more steplike in shape being very asymmetric with excitations that extend to much larger energy losses than the extrinsic losses (see Fig. 2). Note that the characteristic asymmetric shape of the bulk plasmon peak is caused by the intrinsic contribution to the bulk plasmon while the extrinsic bulk plasmon has only a small asymmetry towards higher energy loss.

The spectra taken at glancing angles have less intrinsic losses than those at normal emission. The same for the total losses, which is correlated with the decrease of the inelastic mean free path for more shallow emission. This is easily understood since, for glancing angles the electron loses more energy (to extrinsic excitations) in the vacuum above the surface where it interacts for a longer time with the electrons in the solid compared to an electron being emitted normal to the surface. Therefore the relative contribution of intrinsic excitations decreases with increasing emission angle. This is also likely to be the explanation why the surface excitations are almost purely extrinsic for all angles of emission because the extrinsic excitations that take place as the electron travels in the vacuum occur mostly at the surface plasmon energy.

IV. CONCLUSIONS

The dielectric description of electron energy losses in photoemission described in detail in Ref. 22 and outlined here reproduces quantitatively the angular dependence of surface and bulk electron losses observed experimentally for the $\text{Al}2s$ photoemission spectra of $\text{Al}(111)$, excited with $\text{MgK}\alpha$.² In addition, the model allows one to study the absolute contribution from intrinsic and extrinsic effects in photoemission. It is found that the intrinsic contribution to surface excitations (for the case studied here) is small and

account for less than $\sim 5\%$ of the total intensity corresponding to surface losses. Regarding bulk plasmon excitations, both extrinsic and intrinsic contributions vary significantly with emission angle. The relative intrinsic contribution to the bulk plasmon is smaller at the largest angles of emission. This is attributed to the relatively larger contribution from extrinsic excitations while the electron travels in the vacuum. This is also the reason why the surface plasmon is almost purely extrinsic. The intrinsic bulk plasmon peak is highly asymmetric to the high energy loss side while the extrinsic

bulk plasmon loss peak is nearly symmetric. It is found that the intrinsic contribution to the bulk plasmon excitation represents $\sim 35\%$ of the intensity at the bulk plasmon position at normal emission while only $\sim 18\%$ at 80° glancing emission.

Finally, it is worth stressing that the calculations made here can easily be used to interpret PES spectra of other materials in terms of intrinsic and extrinsic effects, if their dielectric properties [i.e., $\epsilon(k, \omega)$] are known. $\epsilon(k, \omega)$ may be taken from the literature or it may be determined experimentally by quantitative analysis of REELS.

-
- ¹C. N. Berglund and W. E. Spicer, *Phys. Rev.* **136**, A1030 (1964).
²B. I. Lundqvist, *Phys. Kondens. Mater.* **9**, 236 (1969).
³S. Doniach and M. Sunjic, *J. Phys. C* **3**, 285 (1970).
⁴J. L. Gersten and N. Tzoar, *Phys. Rev. B* **8**, 5671 (1973).
⁵J. J. Chang and D. C. Langreth, *Phys. Rev. B* **8**, 4638 (1973).
⁶P. J. Feibelman, *Phys. Rev. B* **7**, 2305 (1973); *Surf. Sci.* **36**, 558 (1973).
⁷G. D. Mahan, *Phys. Rev. B* **11**, 4814 (1975).
⁸W. J. Pardee, G. D. Mahan, D. E. Eastman, and R. A. Pollak, *Phys. Rev. B* **11**, 3614 (1975).
⁹J. B. Pendry, *Surf. Sci.* **57**, 679 (1976).
¹⁰J. C. Fuggle, D. J. Fabian, and L. M. Watson, *J. Electron Spectrosc. Relat. Phenom.* **9**, 99 (1976).
¹¹D. R. Penn, *Phys. Rev. Lett.* **38**, 1429 (1977); **40**, 568 (1978).
¹²P. Steiner, H. Hochst, and S. Hüfner, *Z. Phys. B: Condens. Matter* **30**, 129 (1978).
¹³R. J. Baird, C. S. Fadley, S. M. Goldberg, P. J. Feibelman, and M. Sunjic, *Surf. Sci.* **72**, 495 (1978).
¹⁴J. E. Inglesfield, *Solid State Commun.* **40**, 467 (1981); *J. Phys. C* **16**, 403 (1983).
¹⁵S. Tougaard, *Phys. Rev. B* **34**, 6779 (1986).
¹⁶D. Chastenet and P. Longe, *Phys. Rev. Lett.* **44**, 91 (1981).
¹⁷S. M. Bose, P. Kiehm, and P. Longe, *Phys. Rev. B* **23**, 712 (1981).
¹⁸S. M. Bose, S. Prutzer, and P. Longe, *Phys. Rev. B* **27**, 5992 (1983).
¹⁹L. Hedin, J. Michiels, and J. Inglesfield, *Phys. Rev. B* **58**, 15 565 (1998).
²⁰L. Hedin and J. D. Lee, *J. Electron Spectrosc. Relat. Phenom.* **124**, 289 (2002).
²¹C. Biswas, A. K. Shukla, S. Banik, V. K. Ahire, and S. R. Barman, *Phys. Rev. B* **67**, 165416 (2003).
²²A. C. Simonsen, F. Yubero, and S. Tougaard, *Phys. Rev. B* **56**, 1612 (1997).
²³F. Yubero and S. Tougaard, *Phys. Rev. B* **46**, 2486 (1992).
²⁴F. Yubero, S. Tougaard, E. Elizalde, and J. M. Sanz, *Surf. Interface Anal.* **20**, 719 (1993).
²⁵F. Yubero, J. M. Sanz, J. F. Trigo, E. Elizalde, and S. Tougaard, *Surf. Interface Anal.* **22**, 124 (1994).
²⁶F. Yubero, J. M. Sanz, B. Ramskov, and S. Tougaard, *Phys. Rev. B* **53**, 9719 (1996).
²⁷F. Yubero, D. Fujita, B. Ramskov, and S. Tougaard, *Phys. Rev. B* **53**, 9728 (1996).
²⁸P. Prieto, F. Yubero, E. Elizalde, and J. M. Sanz, *J. Vac. Sci. Technol. A* **14**, 3181 (1996).
²⁹F. Yubero, V. M. Jiménez, and A. R. González-Elipe, *Surf. Sci.* **400**, 116 (1998).
³⁰F. Yubero, J. P. Espinós, and A. R. González-Elipe, *J. Vac. Sci. Technol. A* **16**, 2287 (1998).
³¹W. de la Cruz, G. Soto, and F. Yubero, *Opt. Mater. (Amsterdam, Neth.) (Amsterdam, Neth.)* **25**, 39 (2004).
³²R. H. Ritchie and A. L. Marusak, *Surf. Sci.* **4**, 234 (1966).
³³J. L. Gervasoni, and N. R. Arista, *Surf. Sci.* **260**, 329 (1992).
³⁴R. H. Ritchie and A. Howie, *Philos. Mag.* **36**, 463 (1977).
³⁵*Handbook of Optical Constants of Solids*, edited by Edward Palik (Academic Press, New York, 1985).